Cenozoic tectono-sedimentary evolution of the northern Turkana Depression (East African Rift System) and its significance for continental rifts

A. Nutz [a,*], T. Ragon [b], M. Schuster [c]

[a] *Centre Européen de Recherche et d'Enseignement des Géosciences de l'Environnement, Aix-Marseille Université, CNRS, IRD, Collège de France, INRAE, Aix en Provence, France*
[b] *Seismological Laboratory, California Institute of Technology, Pasadena, CA, USA*
[c] *Université de Strasbourg, CNRS, Institut Terre et Environnement de Strasbourg, UMR 7063, 5 rue Descartes, Strasbourg F-67084, France*

ARTICLE INFO

ABSTRACT

Rifting is an emblematic facet of continental drift and its early stage (i.e., stretching phase) is pivotal to be fully characterized and understood because it then conditions all subsequent stages of the break-up cycle. Although the final architectures of rifted margins have been extensively documented and discussed over the past decades from a wide range of examples and from multiple surface and sub-surface data, the complete evolution of the stretching phase itself remains mostly illustrated from analogue and numerical models and more rarely from real case studies and field evidences. The northern Turkana Depression (Cenozoic East African Rift System) stands as a key natural example to investigate every stage of the evolution of a stretching phase, as it provides almost ∼30 Ma of rift evolution from its initiation to present-day. In this study, we combine field analyses and seismic reflection data to characterize every stage of this tectono-sedimentary evolution, with a focus on the, rarely observed, surface rupture initiation and tectonic decay. In particular, we show rifting initiates with the reactivation of non-optimal inherited structures, progresses with their abandonment during the development of long and wide grabens or half-grabens, and locally terminates with the development of a post-tectonic flexural sag, synchronously to the migration of the locus of brittle deformation to an adjacent area where starts a similar cycle. Our observations allow us to nuance commonly accepted generic rift evolution models, and to discuss possible geodynamic controls on fault evolution and strain migration. We propose a field-based alternate conceptual evolution model for rift systems sharing common characteristics with the northern Turkana Depression such as abundant inherited basement structures, thin and hot lithosphere and a low to moderate magmatism.

1. Introduction

Initiation and evolution of continental rift systems mark the first phase of a continental break-up cycle (Lavier and Manatschal, 2006; Peron-Pinvidic et al., 2013). Referred to as the "stretching phase", this phase is characterized by the development of distributed grabens and/or half-grabens that accommodate relatively minor amounts of extension. Later in the continental break-up cycle, deformation localizes on detachment faults, which affect both the upper and lower crust, allowing crustal thinning, hyperextension until mantle exhumation and ultimately oceanization. During the break-up cycle, deformation progressively migrates basinward (Lavier and Manatschal, 2006; Peron-Pinvidic et al., 2013; Brune et al., 2014; Pérez-Gussinyé et al., 2020), and precursor continental basins are then successively abandoned and capped by post-tectonic sediments (i.e. the so-called "sag deposits"). At the final stage, areas that hosted deformation during the stretching phase classically form the proximal domain of rifted margins (Lavier and Manatschal, 2006; Peron-Pinvidic et al., 2013).

Understanding the evolution of continental rift systems during the stretching phase is fundamental, as it exerts a prime control on the evolution of subsequent stages of the continental break-up cycle, in particular on the potential location of subsequent detachment faults (Naliboff et al., 2017). The development of continental rift systems is driven by the interplay of several mechanisms, the most critical ones being the tectonically induced stress field and the sub-crustal flows (e.g., Ziegler and Cloetingh, 2004), which are

A. Nutz, T. Ragon and M. Schuster

balanced by the strength, viscosity and thermal state of the lithosphere (e.g., Tetreault and Buiter, 2018), the related volume of extruded magma (e.g., Muirhead et al., 2016) and the feedbacks with surface processes (e.g., Olive et al., 2014; Theunissen and Huismans, 2019) or any preexisting lithospheric heterogeneity (e.g., Brune et al., 2017). Several conceptual (e.g., Prosser, 1993; Morley 1999, 2002, 2016; Gawthorpe and Leeder, 2000; Cowie et al., 2005; Phoosongsee and Morley, 2019) and numerical (e.g., Gupta et al., 1998; Cowie et al., 2000; Richter et al., 2021) models describe the initiation and evolution of continental rift systems. For some of them, the rift initiates with small, isolated and spatially distributed extensional basins that develop with an orientation orthogonal to the direction of extension, bordered by high-angle normal faults accumulating limited displacement. With the increase in tensional stresses, isolated fault segments link together in a few major faults of similar orientation, where the strain then localizes to form long and wide basins that accumulate important volumes of sediment. For others, normal faults establish their near-final lengths early in their slip history, after which they grow mainly by displacement accrual (Morley 1999, 2002; Childs et al., 2003; Rotevatn et al., 2019). In both cases, the initiation and the subsequent evolution of wide and long basins record the transition from the initiation phase to the rift climax phase, characterized by maximal strain rates (Prosser, 1993). Commonly, peripheral portions of basins are then progressively abandoned, while active strain migrates inward the rift due to the creation of new intra-basinal faults (Morley, 1994; Goldsworthy and Jackson, 2001; Corti et al., 2013; Wedmore et al., 2020) although in some rift systems, most of the extension remains accommodated by the initial border faults (e.g., Muirhead et al., 2019). Subsequently, during the later post-tectonic phase (*sensu* Prosser, 1993), subsidence, which is no longer tectonically-controlled, becomes mainly sustained by the thermal relaxation of the lithosphere, leading to the long-term development of a flexural sag basin (e.g., Kusznir et al., 1991, 1995). Continental rift evolution has been remarkably well-documented in various basins (e.g., Nottvedt et al., 1995; Gawthorpe et al., 2003; Bell et al., 2018; Ford et al., 2017; Gawthorpe et al., 2018), with special mention to those developed in the East African Rift System (EARS, Morley et al., 1999; Ebinger, 2005; Corti, 2009; Scholz et al., 2020 among others). In parallel, evolutionary scenarios for complete break-up cycles, including the stretching phase, have been proposed from several numerical and analogue modeling (Corti, 2009; Agostini et al., 2011; Brune et al., 2014; Finch and Gawthorpe, 2017; Corti et al., 2019 among others).

However, systematics- in the evolution of rift systems during the stretching phase, from the initiation of surface rupture to the post-tectonic evolution, have rarely been illustrated from a single, natural and active case study. Possible reasons for this lack of knowledge are that complete archives documenting this evolution are rarely exposed or easily observable as they are buried under several kilometers of sediments, and their numerical modeling remains limited by the current resolution of our models (e.g., Brune, 2019; Richter et al., 2021). Here, building on the example of the northern Turkana Depression (EARS), documented by both surface and sub-surface data, we describe the tectono-sedimentary evolution of a continental rift system spanning some 30 Ma, from the initial surface rupture to the subsequent establishment of the post-tectonic phase. We then propose systematics in the evolution of the stretching phase for regions which share characteristics with the northern Turkana Depression, namely abundant inherited basement structures, a thin and hot lithosphere and a poor to moderate magmatic activity. By this way, we bring some nuances to existing evolution models for magma-poor rift systems and discuss possible geodynamic drivers on continental rift evolution.
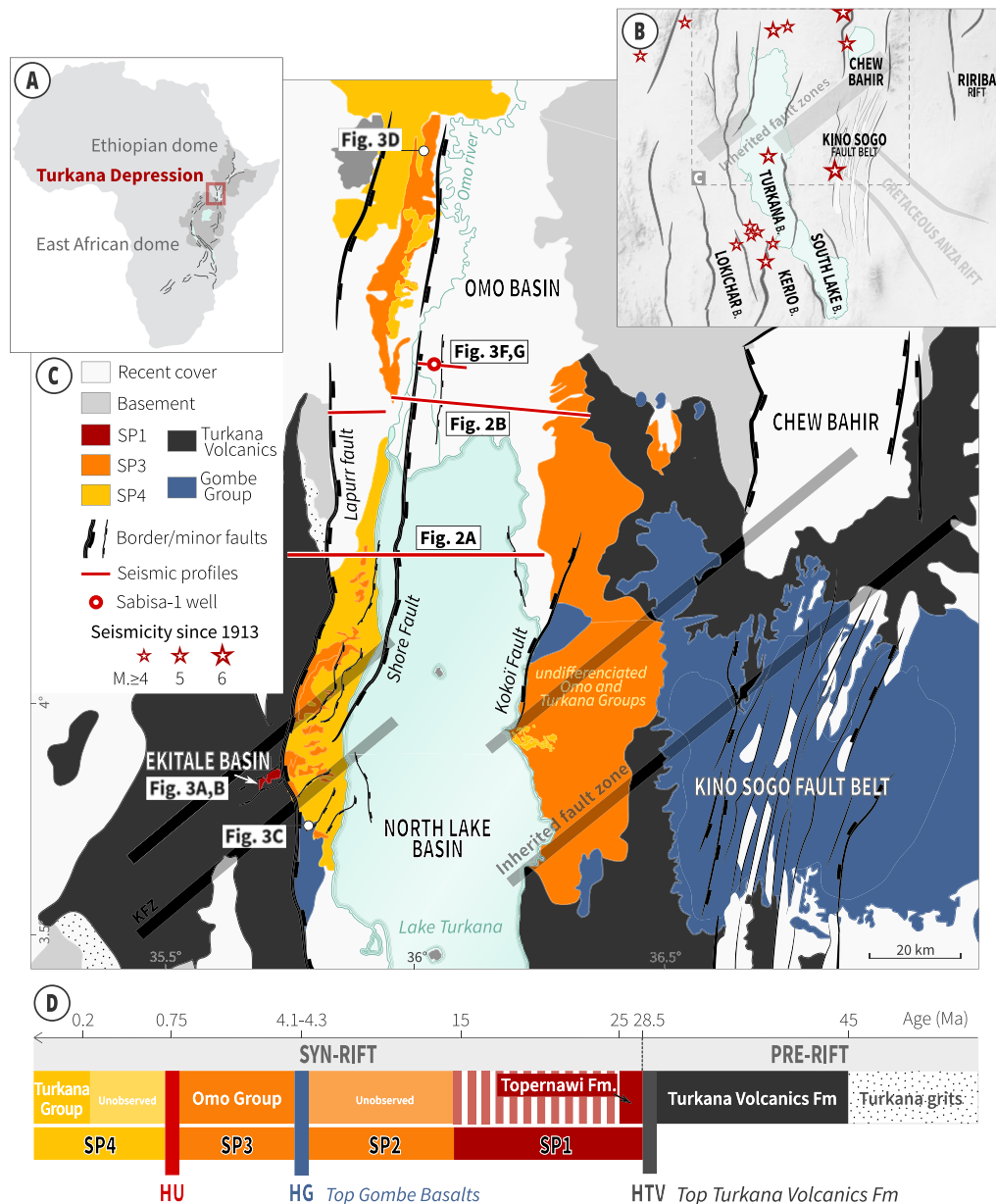
2. The Turkana Depression

The Turkana Depression forms a 200-km-wide lowland that connects the Ethiopian and the Kenyan rifts (Fig., 1A). The Turkana Depression is made of a series of juxtaposed N-S striking half-grabens in the southern part with a low elevation of the rift shoulders, and a single half-graben or asymmetric graben in the northern part, bounded by relatively high rift shoulders. Unlike the 40-km-thick crust of the Ethiopian and Kenyan plateaus (e.g., Benoit et al., 2006), the depression is characterized by a particularly thin crust of ∼20 km right below Lake Turkana (Sippel et al., 2017), partly inherited from the Early Cretaceous rifting in the Anza Basin and early Paleogene emplacement of the South Sudan rifts (Morley, 1999).

Since the Late Eocene, the Turkana Depression experienced 35–40 km of total extension (Hendrie et al., 1994) in the E-W direction (Morley et al., 1999; Vétel and Le Gall, 2006), accompanied with intense volcanism from ca. 45 to 27 Ma, in particular with the emplacement of extended thick traps in the northern part (Rooney, 2017), forming the Turkana Volcanics Fm (Fig. 1C; Bellieni et al., 1981). The earliest manifestation of Cenozoic syn-rift faulting took place in the southern Turkana Depression and corresponds to the opening of the Lokichar basin (Morley et al., 1999) at ca. 35 Ma (Boone et al., 2018). The deformation is then supposed to have progressively migrated eastward, as expressed by the successive opening of the Kerio, South Lake and Turkana Basins (Fig. 1B; Morley, 1999). In the northern Turkana Depression, the first sign of surface rupture is dated at ca. 28.5 Ma with the opening of micro-basins (Ragon et al., 2019). Currently, regional extension rates reach 4–5 mm/year, highest rates are located east of the modern Lake Turkana while extension rates seem to be very modest to the west (e.g., Knappe et al., 2020).

While the Turkana Depression has undergone intense volcanism during Eocene and Oligocene periods (Schofield et al., 2020; Morley, 2020), Morley (2020) suggests dikes accounted for only a minor portion (<2%) of the extensional strain in the region. In the following, we use volcanic levels as stratigraphic markers, but we thus assume magmatic emplacement is a consequence, and not a driving factor, of the tectonic evolution of the region, and we do not focus on the interplay between magmatism and tectonism.

3. Data used in this study

Combination of field analyses and seismic reflection data allowed us to describe and interpret the Cenozoic rift evolution in the northern Turkana Depression, from Oligocene pre-rift conditions to present-day. Field analysis, including geological mapping, structural and sedimentological analyses, were conducted during four surveys between 2014 and 2016. In this contribution, we present in detail two key tectono-sedimentary sections (Fig. 2) across the North Lake and the Omo Basins (Fig. 1), hereafter named the Lowarengak and Omo sections, respectively. They result from the compilation of published seismic data and own field observations. Extensive on- and offshore 2D seismic reflection data acquired by Tullow Oil and partners between 2010 and 2014 were compiled from corporation reports published between 2013 and 2015 (Africa Oil Reports). Additionally, a Master of Science thesis (Alemu, 2017) provides seismic lines in the Omo Basin acquired during the same geophysical campaign. Database was completed with offshore lines from the 1984 PROBE project (published in Dunkelman et al., 1989) and data of the AMOCO project (published in Morley et al., 1999).

Fig. 1. Tectonic and geological background of the northern Turkana Depression and surrounding areas. (A) Location of the Turkana Depression within the East African Rift System (EARS), at the junction of the Ethiopian and Kenyan rifts. (B) Simplified structural map of the Turkana Depression, Chew Bahir basin, Kino Sogo Fault Belt and Ririba rift, overlaid with recent M>4 earthquakes (1913 to present, USGS NIEC Catalog; Ambraseys and Adams, 1991). Fault geometries adapted from Ragon et al. (2019) and Vétel and Le Gall (2006). (C) Geology of the northern Turkana Depression and surrounding regions, modified from Ragon et al. (2019). The Turkana Volcanics Fm (dark gray) cover the rift shoulders, while outcropping sediments mainly consist in the Plio-Pleistocene and Holocene Omo and Turkana Groups. Faults and inherited highly faulted zones are presented. Reconstructed tectono-sedimentary sections are located. (D) Simplified lithostratigraphic chart of the northern Turkana Depression. Syn-rift sedimentary infill is divided into four sediment packages (SP1-4), separated by 3 main horizons: HTV is the top of the Turkana Volcanics Fm, HG the top of the Gombe Group, and HU a basin-scale unconformity.

4. Evolution of the northern Turkana Depression during the Cenozoic rifting

From Oligocene until present-day, periods of sedimentation and volcanic events have succeeded in the northern Turkana Depression, coevally to the rift evolution (Fig. 1C). In this context, four distinct sediment packages (SP1-4) and two significant volcanic units (HTV and HG) allow us to decompose the Cenozoic tectono-sedimentary evolution recorded in the area.

4.1. Pre-rift conditions and syn-tectonic initiation (prior to 25.5 Ma)

In the northern Turkana Depression, the Turkana Volcanics Fm (Fig. 1C) is considered as pre-rift (Morley et al., 1999; Ragon et al., 2019) as it does not show evidence for syn-depositional extension. This formation includes up to 3 km thick Eocene to Oligocene lava flows intercalated with pyroclastic deposits and frequent paleosoils. The spatial extent of the Turkana Volcanics Fm (HTV, Fig. 2A) is, in places, difficult to constrain on available seismic transects, but is well exposed on the current rift shoulders (Fig. 1C).

Earliest evidences of surface ruptures associated with the Cenozoic rifting took the form of isolated kilometer-scale basins (referred to as micro-basins, Ragon et al., 2019) that developed at the top of the Turkana Volcanics Fm at around 28.5 Ma, currently still observable on the western rift shoulder of the North Lake Basin (Fig. 1B, 3A and B). Sediments infilling these micro-basins (SP1) consist in >70 m thick fluvial, lacustrine and pyroclastic deposits
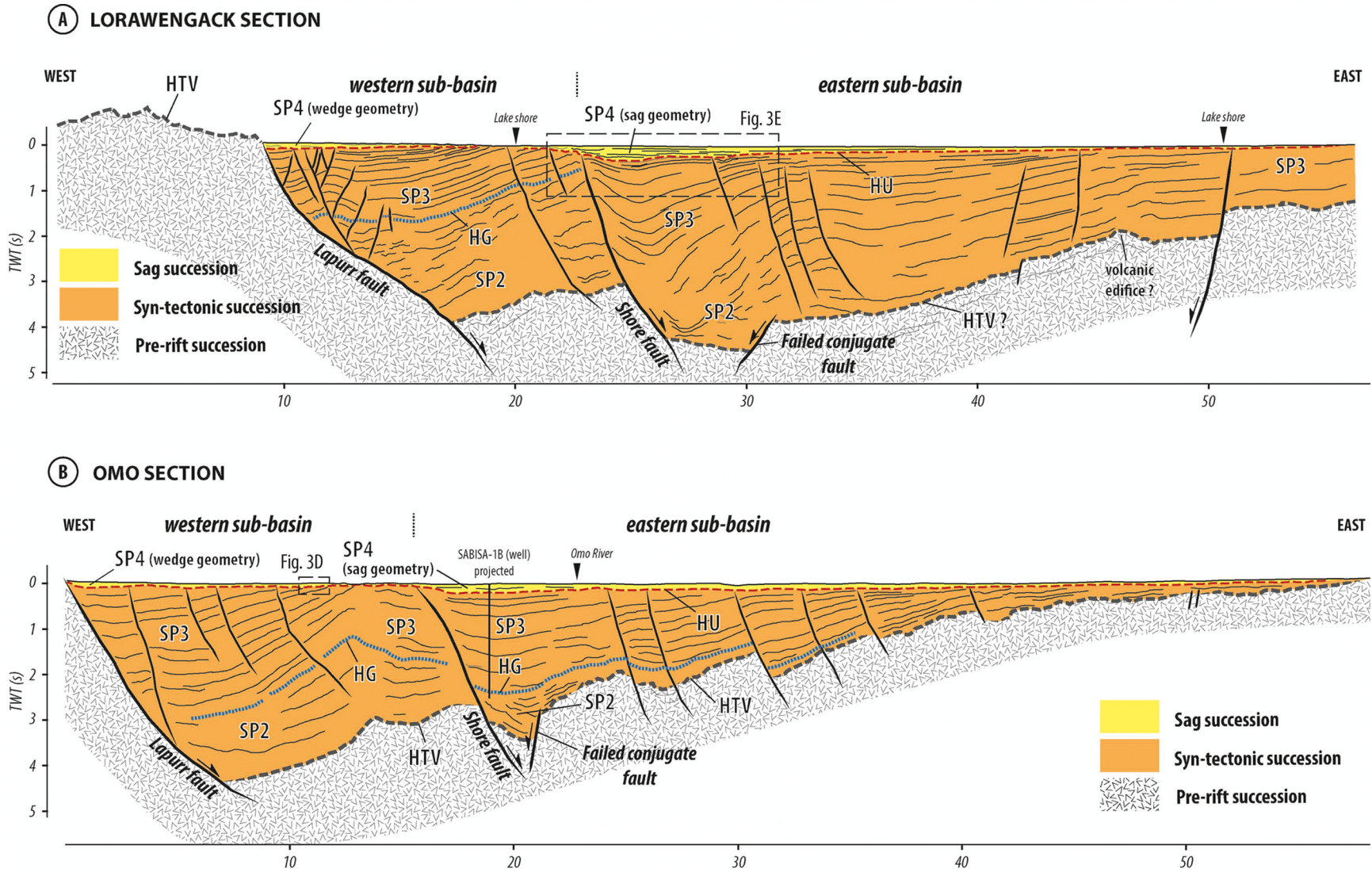
Fig. 2. Reconstructed basin-scale tectono-sedimentary sections of the northern Turkana Depression based on the compilation of published and unpublished seismic sections and field observations (see Fig. 1C for their locations).

A. Nutz, T. Ragon and M. Schuster

revealing limited subsidence and thus limited fault displacements. Such micro-basins are oriented SW-NE, a non-optimal direction regarding the classical E-W oriented extension during the Cenozoic (Morley et al., 1999; Vétel and Le Gall, 2006). Ragon et al. (2019) showed that these micro-basins have developed along a highly faulted zone (i.e., the Kataboi Fault Zone), considered as inherited from previous tectonic events (Vétel and Le Gall, 2006). These authors evidenced that their evolution has mainly been driven by the reactivation of pre-existing inherited structures through oblique extension.

4.2. Syn-tectonic climax (14-0.75 Ma)

The progressive opening of the North Lake and Omo Basins due to the activation of the optimally oriented Lapurr Fault (Fig. 1B) started at ca. 14 Ma (Boone et al., 2018). Initiation of these basins might have followed either a period of tectonic quiescence between 25 and 14 Ma, or a period during which non-optimal micro-basins may have continued to develop even if they are not currently observed neither at exposure nor in seismic profiles. Anyhow, if sedimentation occurred during this period, it was likely scarce and localized in scattered small depocentres.

Between 14 to 4.3 Ma, sediments (SP2) deposited in the North Lake and Omo basins are not exposed, but observed on some portions of seismic lines (Fig. 2). SP2 is topped by the Gombe Group (horizon referred to as HG), which consist in basalts, up to 200 m thick (Fig. 3B) originated from a major volcanic event that occurred in the northern Turkana Depression between ~4.3 and ~3.8 Ma (Haileab et al., 2004). In the Omo section (Fig. 2B), a 50 m thick basalt layer is observed in the Sabisa-1B well from ~1840 and ~1890 m below surface (projected on Fig. 2B; Alemu, 2017; Africa Oil Reports, 2013–2015); this basalt layer is dated as Early Pliocene (Africa Oil Reports), and thus we attribute it to the Gombe Group. Sediments underlying HG thus belong to SP2. Where syn-rift strata are the thicker, SP2 seems to represent about 50–60% and about 30% of the sedimentary infill in the North Lake and the Omo basins, respectively (Fig. 2). This reveals that mean accommodation creation rate was much lower between 14 and 4.3 Ma than during posterior sedimentation of SP3 in both basins.

Directly above HG is the Omo Group (SP3, Fig. 1C, 2, 3) which includes alluvial-fluvial to lacustrine sediments dated between ~4.1 and ~0.75 Ma (McDougall et al., 2012) and currently well exposed around modern Lake Turkana (de Heinzelin, 1983; Feibel, 1988; Nutz et al., 2017, 2020). In both sections (Fig. 2), SP3 is bounded by the Lapurr fault to the west. SP3 represent about 70% and 40–50% of the sedimentary infill in the Omo and the North Lake basins (Fig. 2) indicating that accommodation creation rate significantly increases from the Lower Pliocene in both basins. Around 20 km eastward the Lapurr fault, limited antithetic faults are observed, affecting pre-rift strata and a portion of SP2. They correspond to the conjugate normal faults that developed during the initiation of the graben, subsequently abandoned to form the observed half-graben system ("failed conjugate faults" sensu Scholz and Contreras, 1998). Additionally, SP3 is affected by an important intra-basinal normal fault, referred to as the Shore Fault (Fig. 1B, 2). Eastward, SP3 is bounded by an antithetic normal fault to form an asymmetric graben (Lowarengak section, Fig. 2A) or progressively pinches out, showing a typical half-graben geometry (Omo section, Fig., 2B). SP3 reflectors show wedge geometries associated with both the Lapurr and the Shore faults, interpreted as growth strata delineating a western and an eastern sub-basin genetically associated with the activity of the two different faults. At second-order, the two sub-basins are affected by minor intra-basinal normal faults. In the western sub-basin, both sections show that SP3 is tilted and displays toplap terminations sealed by SP4 (Fig. 2 and 3) revealing that this sub-basin was no more active, rotated and
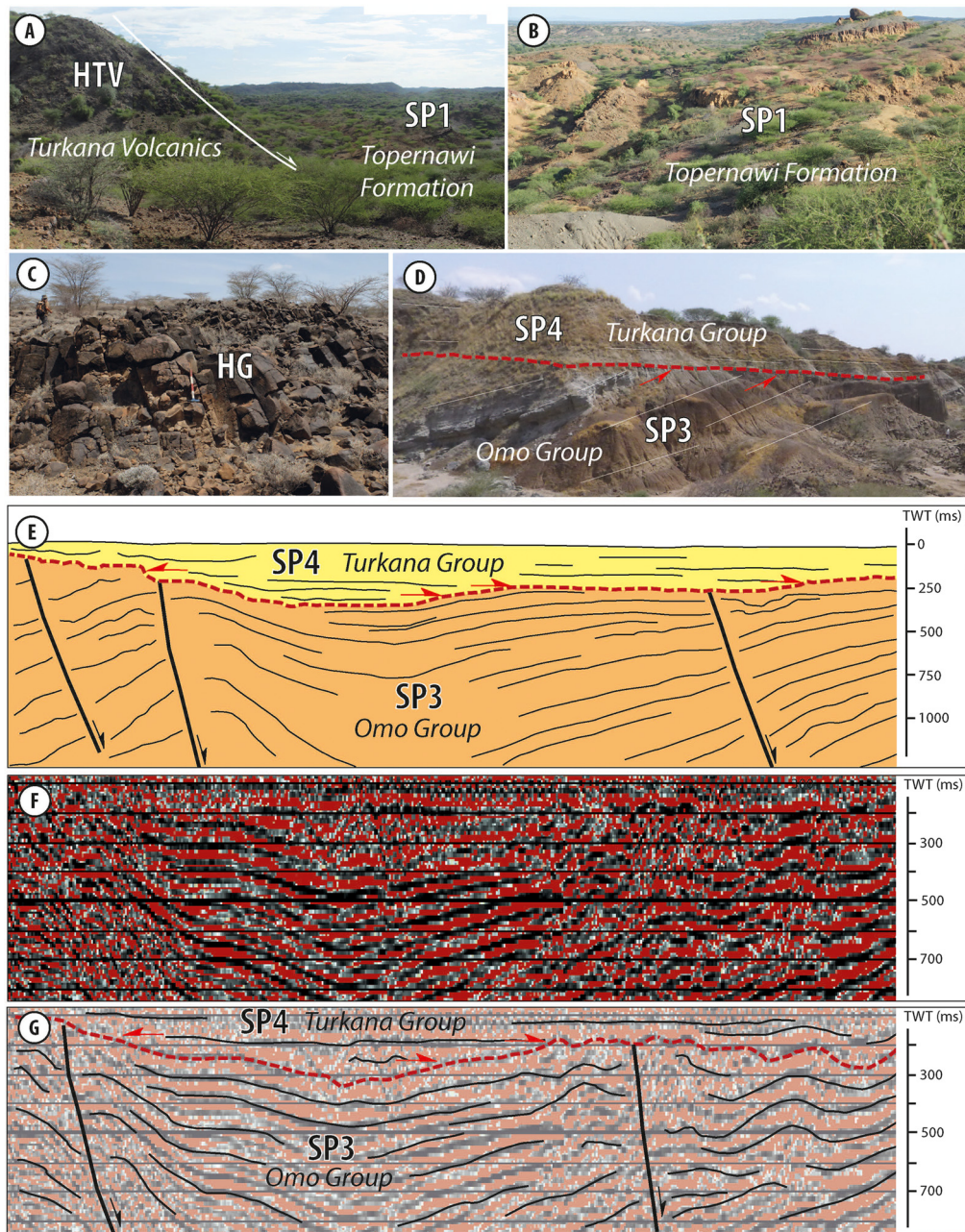
eroded before the onset of SP4 deposition. In contrast, even if angular unconformity (HU) between SP3 and SP4 is visible in the eastern sub-basin (Fig. 2 and 3E, F and G), no erosion of SP3 reflectors is observed.

After 14 Ma, normal faults developed according to an optimal direction and a large amount of sediments have accumulated in the North Lake and Omo basins. Prior to ca. 4.3 Ma, even if the age cannot be more precisely determined, the initiation of the Shore Fault led to the segmentation of the North Lake and the Omo basins in two distinct sub-basins, namely the western and eastern sub-basins. Subsequently, the western sub-basin interrupted, expressing an inward migration of the deformation to the eastern sub-basin and thus a narrowing of the rift system. Youngest sediments included in SP3 in the western sub-basin are ~0.75 M years old in the North Lake Basin and ~1.2 M years old in the Omo Basin, evidencing that the narrowing occurred diachronously, shortly after 0.75 Ma and 1.2 Ma in the North Lake and Omo basins, respectively. Thus, from 0.75 Ma, active rifting became controlled by the Shore Fault (Fig. 2) while the Lapurr fault interrupted.

In parallel, the Chew Bahir Basin (CBB, Fig. 1B and C) and Kino Sogo Fault Belt (KSFB, Fig. 1B and C) were active east of the northern Turkana Depression. Indeed, while the precise chronology of the Chew Bahir rift onset remains poorly constrained (Ebinger et al., 2000), rifting was likely continuous from mid-Miocene to recent times (Pik et al., 2008), although some authors suggest rifting in the south was mostly Plio-Quaternary (Vétel et al., 2005). To the southern continuation of the Chew Bahir rift, the KSFB crosscuts a volcanic unit dated at 3 Ma in the locality, in a swarm of juxtaposed narrow N-S oriented series of horsts and grabens (Vétel et al., 2005). Even if the age cannot be precisely determined, the development of the KSFB thus started after 3 Ma (Vétel et al., 2005). Vétel et al. (2005) conclude that the evolution of the KFSB has been controlled by structural inheritance, either from basement fabrics or from prior unobserved Cenozoic rifted structures, with a potential effect of volcanic doming.

4.3. Post-tectonic sag and lateral migration (<750 ka)

The Turkana Group (SP4, Fig. 1C, 2, 3) overlays the Omo Group (SP3). Well exposed around modern Lake Turkana, SP4 consists in fluvial to lacustrine sediments corresponding to the Kibish and Galanaboi Fms (Figs. 1 and 3; Butzer, 1971; Owen and Renaut, 1986; Nutz and Schuster, 2016; Schuster and Nutz, 2018), in places intercalated with volcanic deposits. SP4 reaches more than 120 m thick in the Omo Basin, the uppermost ~100 m having been deposited during the last 200 ky (McDougall et al., 2005). SP4 is well delineated onshore, where SP3 toplaps SP4, forming a particularly well-expressed unconformity (Fig. 3D). Offshore, SP4 consists in continuous and parallel reflectors that seal the normal faults which crosscut SP3 (Fig. 2, 3E, F and G). In the western sub-basin, SP4 slightly thickens towards the Lapurr fault showing a subtle wedge geometry, and unconformably overlays SP3 (Fig. 2). In the eastern sub-basin, SP4 passively infills SP3's paleotopography as evidenced by onlap terminations (Fig. 2, 3E, F and G), while it laterally pinches out on both sides, revealing a classical sag geometry. The unconformity (HU), marking the transition between SP3 and SP4, is well-defined in the North Lake and Omo basins, both on seismic lines and on outcrops (Fig. 3C, D and E). HU is interpreted as a major basin-scale surface as it is correlated with an angular unconformity frequently observed between 300 and 150 ms (TWT) in several of the seismic profiles (lines 302; 307, 330 and 332) of the northern Turkana Depression acquired by PROBE (Dunkelman et al., 1989), yet unaddressed by the authors. In the eastern sub-basin, SP4 evidences a basin-scale transition from a fault-driven to a flexural subsidence, revealing the transition from a syn- to post-

Fig. 3. Field photographs and close-up views of seismic profiles. (A) Border faults of the Ekitale micro-basin separating volcano-sedimentary rocks of the Topernawi Formation (SP1) and the Turkana Volcanics Formation onto the current rift shoulder of the North Lake Basin (for details, see Ragon et al., 2019). (B) Large view of the Topernawi Fm in the Ekitale basin (for details see Ragon et al., 2019). (C) Gombe basalts exposed in the western part of the North Lake Basin. On tectono-sedimentary sections, they are labeled as HG. (D) Outcrop showing the angular unconformity between SP3 and SP4 (HU) in the western sub-basin of the Omo Basin (location on Fig. 2B). (E) Interpreted section displaying the angular unconformity between SP3 and SP4 (HU) in the North Lake Basin, east of the Shore Fault (location on Fig. 2A). (F) Raw seismic line SO-22 from Alemu (2017) (see location Fig. 1C). (G) Interpreted seismic line SO-22 showing SP4 infilling the paleotopography of SP3 in the eastern sub-basin of the Omo Basin and revealing a non-erosional angular unconformity.

tectonic evolution. In the western sub-basin, the slight wedging of SP3 suggests a limited activity of the Lapurr Fault at least after 0.75 Ma, indicating a residual syn-tectonic activity in the northern Turkana Depression. However, the dominant flexural deformation advocates for low local strain and extension rates in the Turkana Depression, for at least 200 ka, the transition from tectonic to flexural subsidence being posterior to 1.2 Ma in the Omo Basin and to 0.75 Ma in the North Lake Basin, and anterior to 0.2 Ma in both cases.

Plate kinematic models of the EARS suggest steady extension at ~4–5 mm/yr in the Turkana area for the last ~3 Ma (Stamps et al., 2008; Melnick et al., 2012) and the Turkana Depression is still home to active deformation, as attested by recent seismic activity (Fig. 1, NEIC catalog from 1900 to present). However, Knappe et al. (2020) show local extension rates are very low west of Lake Turkana, and reach 4–5 mm/yr further east. Moreover, recent seismicity in the KSFB and Chew Bahir rift (Fig. 1) evidences active deformation east of the Turkana area. For at least 200 ka, reduced local strain and extension rates in the northern Turkana Depression, in opposition to larger strain and extension rates to the east support an eastward migration of the syn-tectonic deformation. We propose that the development of the KFSB after 3 Ma localized the deformation revealing that this migration started during the northern Turkana Depression rift climax, even if the precise tim-

ing remains unknown. Such eastward migration of the strain has already been conjectured by several authors, albeit never dated (Hendrie et al., 1994; Morley, 1994; Morley et al., 1999, 2020; Ebinger et al., 2000; Vétel and Le Gall, 2006; Corti et al., 2019). Here, we demonstrate this eastward migration was ongoing after 3 Ma and was almost completed at least for 200 ka, as, since then, the syn-tectonic deformation almost totally interrupted in the northern Turkana Depression and was replaced by a flexural deformation. This migration is thus responsible for a concomitant evolution of a post-tectonic sag in the northern Turkana Depression and a syn-tectonic basin in the KSFB.

5. Evolution of the northern Turkana Depression: an alternative rift model?

Numerical simulations suggest that increase in extension velocity characterizes transitions between the different phases of the break-up cycle (Brune et al., 2016; Ulvrova et al., 2019). Pre-rift stresses progressively build-up until a phase of "slow" rifting (at steady-stresses) is reached, which corresponds to the stretching phase that can last up to ∼30 Myr. Then, a 10 to 20 Myr-long period of increase in extension rates (coeval with a stress drop) that occurs during the thinning and exhumation phases, synchronously with a transition from distributed to localized deformation, leads to continental break-up and oceanization. However, little is known about responses of continental rift systems to the stress build-up and its stabilization during the "slow-rifting" stage. The transition from rift initiation to rift climax is commonly thought to be implied by the progressive increase in the tensional stress (e.g., Cowie et al., 2005), while the post-tectonic stage is expressed by lower extension rates. In the following, we investigate the factors that affect, or manifest, the tectono-sedimentary evolution of extensional basins during the stretching phase. We focus on the spatial and temporal evolution of the stress regime, and the potential impact of lithospheric inheritance, confirming that the development of rifts comparable to the northern Turkana Depression is driven by expected increases in tensional stresses and bulk extension, modulated by structural inheritances. Ultimately, we propose an alternate evolution model (Fig. 4) for the development of rift basins in a Northern Turkana Depression-like context, tempering typical views of the rifting initiation and of the transition from climax to early post-tectonic deformation. We propose that the repetition of the above presented cyclic evolution interspersed by repeated lateral migrations forms adjacent and diachronous rift basins, altogether constituting a particular rift system. Finally, based on this evolution model, we also discuss which factors could promote a similar evolution in other rift basins.

5.1. Rift initiation: from oblique micro-basins to optimal wide and long basins
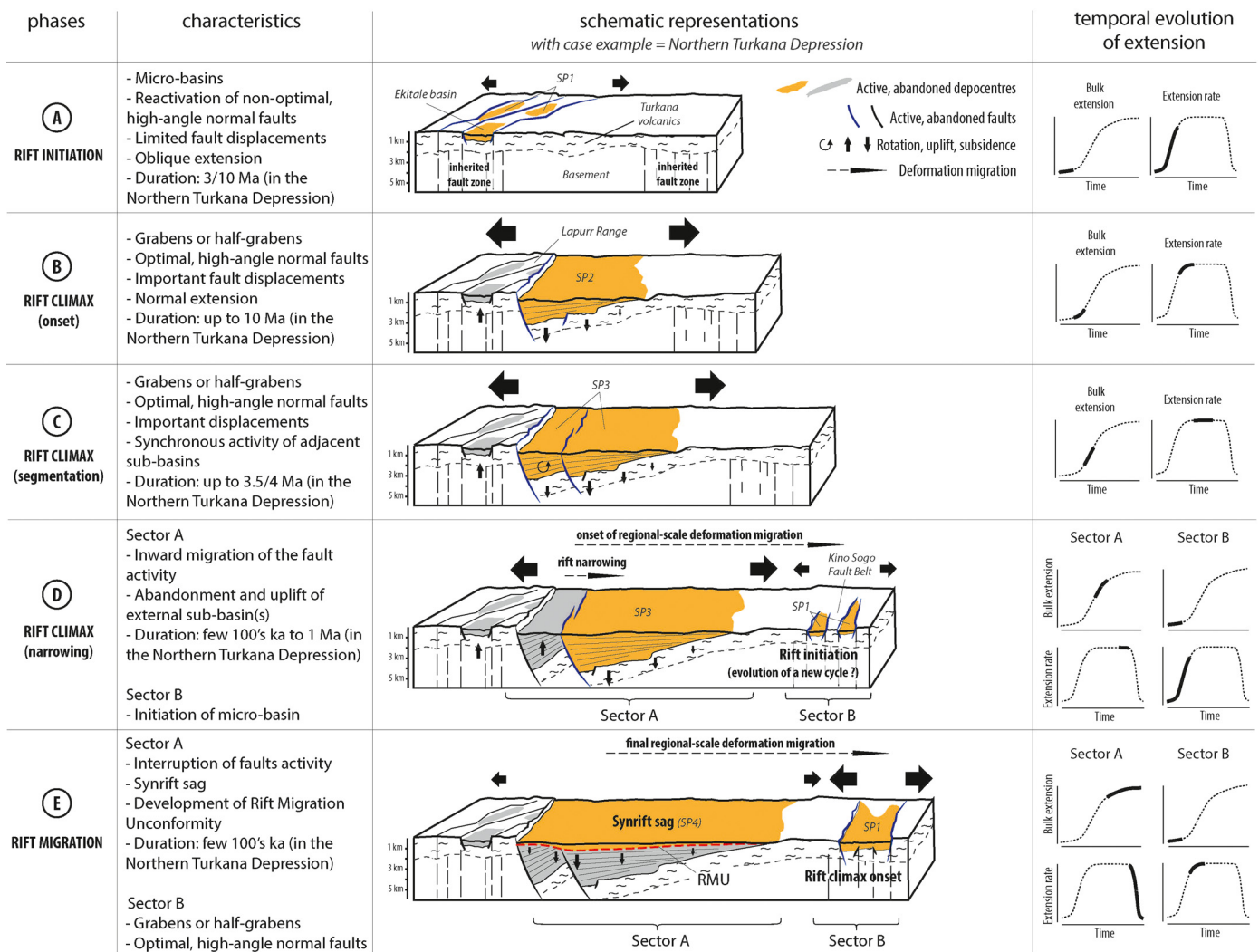
In extensional settings, the Andersonian theory (Anderson, 1905) supposes that normal faults develop in an orthogonal direction to the least compressive stress (σ_3), the greatest principal stress (σ_1) being vertical. However, the differential stress (σ_1-σ_3) required to reactivate non-optimally oriented pre-existing faults is lower than that necessary to initiate an optimal σ_2 parallel failure (e.g., Morley et al., 2004). Hence, at low tensional stress, reactivation of pre-existing structures is favored over the creation of new optimally oriented structures (e.g., Morley et al., 2004). When pre-existing structures are not optimally-oriented compared to the stress field, reactivation takes the form of oblique extension (Morley et al., 2004; Duclaux et al., 2020). With increasing differential stress, primarily reactivated structures cannot accommodate the strain anymore and new optimally oriented failure initiates.

Most continental rifts develop in regions where anterior geodynamic events have produced inherited crustal heterogeneities. We thus propose that, in preamble to the growth of optimal segments and their subsequent linkage (Prosser, 1993; Gawthorpe and Leeder, 2000), rift initiation can be expressed by the preliminary activation of non-optimal inherited structures through oblique rifting, favored by a phase of low tensional stresses (Fig. 4A). Based on Ragon et al. (2019), we suggest that limited extension rates during this initiation phase lead to the reactivation of inherited fault zones and the development of km-scale narrow and thin basins. The more abundant the basement inherited fabrics are, the easier micro-basins form. Nevertheless, in the absence of either inherited fabrics or easily activated pre-existing structures, this phase will be absent of the rift evolution. Such discrete early syn-tectonic micro-basins remain mostly unnoticed, as probably buried under a thick pile of posterior deposits and thus non-observable in most of rift systems, at the exception of some rare examples which developed on future rift shoulders (Ragon et al., 2019). The duration of this initiation phase is poorly constrained, but in the Turkana Depression, it spanned at least 2.5 Myr and at most 13.5 Myr. The subsequent transition from oblique to orthogonal rifting is the direct consequence of an increase in the tensional stresses. Oblique micro-basins are then abandoned, and the formation of new optimally-oriented structures is favored, coeval with a significant increase in extension rate, which manifests the transition from rift initiation to rift climax (Fig. 4B).

5.2. Rift climax: onset, segmentation and narrowing

The northern Turkana Depression evolved as a perfect textbook case during most of its climax, following typical evolution presented in existing models (Prosser, 1993; Gawthorpe and Leeder, 2000; Cowie et al., 2005). In early times of the rift climax, optimally-oriented structures developed forming major border faults that accommodate most of the strain, large displacement rates likely provoking consequent footwall topography (Fig. 4B). Intra-basinal faults then form in the initial depocentre, and show limited displacements. Progressively, the activity of some intra-basinal faults intensifies, while peripheral faults are still active. A significant part of the extension is accommodated by a localized subsidence in several juxtaposed and synchronous sub-basins marking the segmentation of the initial rift basin (Fig. 4C). The duration of the period characterized by the co-evolution of segmented sub-basins is not well-constrained, but likely spans several million years. Interestingly, similar synchronous activity of juxtaposed sub-basins has already been reported for other basins in the East African Rift System (McCartney and Scholz, 2016).

Subsequently, the gradual attenuation of the initial border fault activity, and finally its complete interruption, leads to the narrowing of the rift system (Fig. 4D). Inward migration of the active faulting results in the uplift and erosion of the peripheral basins, while high displacement rates are accommodated by an intra-basinal fault that progressively becomes the new border fault. Abandonment of border faults and migration of the deformation to intra-basinal faults is attributed to the continued increase in the amount of extension (Corti et al., 2013), and is not related to particular variations in extension rates. Narrowing of rift basins due to the riftward shift in strain accommodation has been extensively studied (Cowie et al., 2005; Ebinger, 2005; Corti et al., 2009) and observed in others rift systems such as the Main Ethiopian Rift (Corti et al., 2013), or the Permian-Triassic East Greenland rift system (Guarnieri et al., 2017). Several successive episodes of inward migration of faulting can occur in a single rift basin, an emblematic example being the Corinth rift (e.g., Ford et al., 2017). A specificity of the northern Turkana Depression is that rift narrowing is contemporaneous to a regional-scale lateral migration of the brittle

Fig. 4. Ideal schematic evolution of a northern Turkana Depression-like rift system during the "stretching phase", from pre-rift to early post-tectonic conditions. Five steps are here individualized, they illustrate a comprehensive time series of the rift system configuration characterized by different combinations of cumulative deformation and extension rate.

deformation (Fig. 4D). Indeed, we show that, after the rift segmentation but before the rift narrowing, a new area of active faulting started a few tens of kilometers eastward, in the KSFB.

5.3. Rift migration: concomitant syn- and post-tectonic systems

In standard rift models, after rift abandonment, the uplifted lithosphere cools down and brings the crust into a thermal subsidence (Kusznir et al., 1991, 1995; Prosser, 1993; Morley and Westaway, 2006). Usually, resulting sag basins, considered as post-rift, develop relatively late in the rift cycle, several million years after the rift climax establishment. However, this traditional view of a post-rift thermal flexure is not applicable to our case study. Indeed, in the northern Turkana Depression, the interruption of the rift climax and the onset of a post-tectonic sag are the result of a regional-scale lateral migration of the syn-tectonic deformation (Fig. 4E). This migration makes coexisting post- and syn-tectonic deformation, revealing the sag is not post-rift; a similar configuration has interestingly already been described in the Central Kenya Rift (Morley, 1994) and in rifts of South China sea (Morley, 2016). Moreover, the lithosphere-cooling origin of the subsidence remains unlikely as continued volcanic activity until late Pleistocene (Morley et al., 1999), and high present-day geothermal gradient (Morley

et al., 1999; Boone et al., 2018) combined with a hot lithosphere (Benoit et al., 2006; Kounoudis et al., 2021) suggest that the crust is hot. In parallel, numerous observations and recent numerical simulations suggest that 50–100 km lateral strain migrations are common during the continental break-up cycle (e.g., Brune et al., 2014; Pérez-Gussinyé et al., 2020). The evolution of the northern Turkana Depression is interestingly well reproduced by simulations of Pérez-Gussinyé et al. (2020), in which migration of the locus of upper crustal strain favors the emplacement of syn-rift sag basins relatively early after the onset of the rift climax, coevally to syn-tectonic sedimentation in adjacent younger basins. The authors also suggest that the migration is at the origin of unconformities (i.e., Rift Migration Unconformities, RMU) in the abandoned rift portion, which find a natural analogue in the major unconformity (HU) that we here identified for the northern Turkana Depression from both field observation and seismic profiles interpretation.

We thus illustrate an active continental rift that experiences the concomitant development of post- and syn-tectonic deformation at regional-scale. This synchronous regional post- and syn-tectonic attitude is made possible by the lateral migration of the brittle deformation to a neighboring region and expressed by a local decrease (or increase, respectively) in extension rates (Fig. 4E). Then, a newly-developed basin initiates in tectonically active regions,

while abandoned basins undergo background flexural subsidence and related sag sedimentation above a RMU (Fig. 4E). Several subsequent regional migratory episodes can occur, forming adjacent and diachronous rift basins, until either the localization of the deformation on detachment faults, marking the onset of the thinning phase (Lavier and Manatschal, 2006; Peron-Pinvidic et al., 2013), or the abandonment of the continental rift.

6. Origin of the regional-scale deformation migration?

In the above presented evolution, we suggest that early minor oblique basins mark the rift onset (Fig. 4A), but are then abandoned as large optimal graben or half-graben develop (Fig. 4B, C, D). Subsequently, optimal basins are abandoned, and the locus of extension shifts to a new zone (Fig. 4E) where the cycle restarts through the development of minor basins (possibly oblique, according to inherited structures). In this cyclic evolution, the abandonment of optimal grabens or half-grabens, and the regional-scale migration of the deformation to an adjacent area, represents a major transition that need to be explained.

Various factors might explain the regional migration in the locus of brittle deformation, which here defines the transition from syn- to post-tectonic stages. Ebinger et al. (1991) and Scholz and Contreras (1998) suggest that the maximum throw of a normal fault can be derived from the effective elastic thickness of the lithosphere. In the Turkana area, this maximum throw would be in the order of ~4 km (Scholz and Contreras, 1998); which broadly corresponds to the throw observed on seismic profiles (Fig. 2). A convincing cause for the lateral migration can thus be that border faults have reached their maximum slip, and became inactive. As a consequence, new structures had to develop in order to accommodate the deformation. The location of new zones affected by brittle deformation is favored by the existence of inherited crustal weakness; in the northern Turkana Depression, the development of the KSFB was favored by the existence of basement fabrics and from prior unobserved Cenozoic rifted structures (Vétel and Le Gall, 2006). Moreover, Cenozoic rifting in the Turkana Depression has been preceded by, and concomitant to, several large magmatic episodes. As such, we cannot rule out the possible role of igneous activity on tectonic processes through the creation of fractures and faults potentially reused during the migration of the strain locus.

7. Which key factors may promote a northern Turkana Depression-like evolution?

The northern Turkana Depression shows a complex tectonosedimentary evolution during the Cenozoic. A combination of few key factors seems to control, at first order, this particular evolution. We propose that inheritance is one of these key factors. Inherited fault zones play a pivotal role in the incipient stages of rifting, as also recently observed in other portions of the EARS (e.g., Wedmore et al., 2020; Wright et al., 2020; Kolawole et al., 2021). Yet, in the Turkana area, preexisting structures and Cenozoic rift-related faults have a clearly distinct orientation, at the difference of many other regions, which may favor the development of non-optimal micro-basins during the initiation phase (Fig. 4A). Combined with the occurrence of inherited structures, an extended lithosphere is another key factor. In the Turkana area, the lithosphere is thin and hot, making the lower crust weak and the crust thin (Sippel et al., 2017). Thinner is the crustal effective elastic thickness, lower is the maximum potential throw of normal faults (Scholz and Contreras, 1998; Corti et al., 2010). Thus, an extended lithosphere makes faster the potential locking-up of normal faults. As a consequence, both the rift narrowing (Fig. 4D) and the regional-scale migration of the deformation (Fig. 4E) are favored with thinner crust and delayed with thicker crust. A weak lower crust has been showed to

affect numerous magma-poor (Type II margins of Huismans and Beaumont, 2011) and magma-rich rifts (Ebinger and Casey, 2001), and is now believed to characterize most of rifts (Clerc et al., 2018). Finally, the poor to moderate magmatic activity is the last key factor. It remains unclear yet what is the contribution of magmatism to the tectonic evolution of the northern Turkana Depression, but the region does not evolve as a magma-rich rift (such as in Afar, Stab et al., 2016) as dykes emplacement did not accommodate significant deformation (Morley, 2020). The presented model might thus define rifts or rifted margins characterized by (i) abundant inherited structures due to previous geodynamic events, (ii) a thin and hot lithosphere and (iii) a poor to moderate magmatism. We propose these parameters particularly characterize areas which experienced multiple, successive continental rift cycles and the absence of major magma production. In contrast, magma-rich rift systems and areas characterized by the presence of a strong lower crust or the scarcity/absence of (non-optimal) inherited structures might prevent the presented evolution.

8. Conclusion

Continental rift systems are the expression of the stretching phase at the beginning of a continental break-up cycle. Understanding their evolution is critical to fully conceptualize the continental break-up, and because they participate to shape the subsequent development of rifted margins (Naliboff et al., 2017). However, the pre-rift, syn-tectonic and post-tectonic syn-rift evolutionary stages of a continental rift system have rarely been illustrated from a single active, natural case. Here, we reconstruct the Cenozoic rifting evolution of the northern Turkana Depression, from a combined analysis of field and seismic reflection datasets.

In areas heavily affected by inherited structures and characterized by a particularly extended and hot lithosphere, and a poor to moderate igneous activity, we propose that the stretching phase can evolve as follows. The stretching phase is initiated by low tensional stresses, which favors the reactivation of non-optimal structures oriented along inherited weaknesses. As such, isolated, narrow and shallow km-scale basins form and accommodate low extension rates. With increasing stresses, reactivated structures cannot accommodate the strain anymore and new optimal failures initiate. This marks the transition to the rift climax, characterized by a drastic increase in extension rates, which results in a shift from oblique to orthogonal rifting. The tectonic activity, localized on major border faults, allows the growth of wide and long optimal grabens and half-grabens in which the sedimentation concentrates. During this rift climax, extension rates rapidly increases and then stabilizes, leading the basin to its segmentation and frequently to its narrowing. A regional-scale migration of the locus of brittle deformation, which can start during the climax, favored by a weak lower crust and/or inherited upper-crustal weaknesses, then allows the synchronous development of juxtaposed post- and syn-tectonic basins. After this migration event, in the initial basin, the climax is followed by the drastic reduction of the tectonic activity and a post-tectonic syn-rift flexural subsidence. This post-tectonic flexure is characterized by a sag sedimentation above a rift migration unconformity, and is associated to a local decrease in extension rates, which otherwise stay steady regionally. The lateral stacking of diachronous basins resulting from successive migration events progressively form a complex rift system, until the development of detachment faults and the transition to the thinning phase of the break-up cycle. Although this cyclic evolution is presented in a continuum, it may be interrupted by some periods of tectonic quiescence, making it rather similar to a multiphase rift evolution.

CRediT authorship contribution statement

A. Nutz, T. Ragon and M. Schuster together conceptualized this manuscript.

A. Nutz wrote the manuscript while T. Ragon and M. Schuster reviewed several times the manuscript during the writing process.

Declaration of competing interest

The authors declare that they have no known competing financial interests or personal relationships that could have appeared to influence the work reported in this paper.

Acknowledgements

References

Africa oil reports. Corporate presentations, 2013 to 2015. https://africaoilcorp.com/investors/corporate-presentations/.

Agostini, A., Bonini, M., Corti, G., Sani, F., Mazzarini, F., 2011. Fault architecture in the main Ethiopian rift and comparison with experimental models: implications for rift evolution and Nubia–Somalia kinematics. Earth Planet. Sci. Lett. 301 (3–4), 479–492. https://doi.org/10.1016/j.epsl.2010.11.024.

Alemu, T., 2017. Seismic reflection studies of South Omo Basin, South western Ethiopia. Master Thesis. Addis Ababa University. 63 pp. http://213.55.95.56/handle/123456789/7766.

Ambraseys, N.N., Adams, R.D., 1991. Reappraisal of major African earthquakes, South of 20°N, 1900–1930. Nat. Hazards 4 (4), 389–419. https://doi.org/10.1007/BF00126646.

Anderson, E.M., 1905. The dynamics of faulting. Trans. Edinb. Geol. Soc. 8 (3), 387–402. https://doi.org/10.1144/transed.8.3.387.

Bell, R.E., Duclaux, G., Nixon, C.W., Gawthorpe, R.L., McNeill, L.C., 2018. High-angle, not low-angle, normal faults dominate early rift extension in the Corinth rift, central Greece. Geology 46 (2), 115–118. https://doi.org/10.1130/G39561.1.

Bellieni, G., Visentin, E.J., Zanettin, B., Piccirillo, E., Di Brozolo, F.R., Rita, F., 1981. Oligocene transitional tholeiitic magmatism in northern Turkana (Kenya): comparison with the coeval Ethiopian volcanism. Bull. Volcanol. 44 (3), 411–427.

Benoit, M.H., Nyblade, A.A., Pasyanos, M.E., 2006. Crustal thinning between the Ethiopian and East African plateaus from modeling Rayleigh wave dispersion. Geophys. Res. Lett. 33 (13). https://doi.org/10.1029/2006GL025687.

Boone, S.C., Seiler, C., Kohn, B.P., Gleadow, A.J.W., Foster, D.A., Chung, L., 2018. Influence of rift superposition on lithospheric response to East African rift system extension: Lapur range, Turkana, Kenya. Tectonics 37 (1), 2017TC004575. https://doi.org/10.1002/2017TC004575.

Brune, S., 2019. Modelling Continental Rift Dynamics. Universität Potsdam.

Brune, S., Corti, G., Ranalli, G., 2017. Controls of inherited lithospheric heterogeneity on rift linkage: numerical and analog models of interaction between the Kenyan and Ethiopian rifts across the Turkana depression. Tectonics 36 (9), 1767–1786. https://doi.org/10.1002/2017TC004739.

Brune, S., Williams, S.E., Butterworth, N.P., Müller, R.D., 2016. Abrupt plate accelerations shape rifted continental margins. Nature 536 (7615), 201–204. https://doi.org/10.1038/nature18319.

Brune, S., Heine, C., Pérez-Gussinyé, M., Sobolev, S.V., 2014. Rift migration explains continental margin asymmetry and crustal hyper-extension. Nat. Commun. 5 (1), 4014. https://doi.org/10.1038/ncomms5014.

Butzer, K.W., 1971. The lower Omo Basin: geology, fauna and hominids of Plio-Pleistocene formations. Naturwissenschaften 58 (1), 7–16. https://doi.org/10.1007/BF00620796.

Childs, C., Nicol, A., Walsh, J.J., Watterson, J., 2003. The growth and propagation of synsedimentary faults. J. Struct. Geol. 25, 633–648.

Clerc, C., Ringenbach, J.-C., Jolivet, L., Ballard, J.-F., 2018. Rifted margins: ductile deformation, boudinage, continentward-dipping normal faults and the role of the weak lower crust. Gondwana Res. 53, 20–40. https://doi.org/10.1016/j.gr.2017.04.030.

Corti, G., Cioni, R., Franceschini, Z., Sani, F., Scaillet, S., Molin, P., Isola, I., Mazzarini, F., Brune, S., Keir, D., Erbello, A., Muluneh, A., Illsley-Kemp, F., Glerum, A., 2019. Aborted propagation of the Ethiopian rift caused by linkage with the Kenyan rift. Nat. Commun. 10 (1), 1309. https://doi.org/10.1038/s41467-019-09335-2.

Corti, G., Ranalli, G., Agostini, A., Sokoutis, D., 2013. Inward migration of faulting during continental rifting: effects of pre-existing lithospheric structure and extension rate. Tectonophysics 594 (Supplement C), 137–148. https://doi.org/10.1016/j.tecto.2013.03.028.

Corti, C., Ranalli, G., Mulugeta, G., Agostini, A., Sani, F., Zugu, A., 2010. Control of the rheological structure of the lithosphere on the inward migration of tectonic activity during continental rifting. Tectonophysics 490, 165–172.

Corti, G., 2009. Continental rift evolution: from rift initiation to incipient break-up in the main Ethiopian rift, East Africa. Earth-Sci. Rev. 96 (1), 1–53. https://doi.org/10.1016/j.earscirev.2009.06.005.

Cowie, P.A., Gupta, S., Dawers, N.H., 2000. Implications of fault array evolution for synrift depocentre development: insights from a numerical fault growth model. Basin Res. 12 (3–4), 241–261.

Cowie, P.A., Underhill, J.R., Behn, M.D., Lin, J., Gill, C.E., 2005. Spatio-temporal evolution of strain accumulation derived from multi-scale observations of Late Jurassic rifting in the northern North Sea: a critical test of models for lithospheric extension. Earth Planet. Sci. Lett. 234 (3), 401–419. https://doi.org/10.1016/j.epsl.2005.01.039.

de Heinzelin, J., 1983. The Omo Group. Koninklijk Museum voor Midden-Afrika, Geologische Wetenschappen. Tervuren.

Duclaux, G., Huismans, R.S., May, D.A., 2020. Rotation, narrowing, and preferential reactivation of brittle structures during oblique rifting. Earth Planet. Sci. Lett. 531, 115952. https://doi.org/10.1016/j.epsl.2019.115952.

Dunkelman, T.J., Rosendahl, B.R., Karson, J.A., 1989. Structure and stratigraphy of the Turkana rift from seismic reflection data. J. Afr.Earth Sci. (and the Middle East) 8 (2), 489–510.

Ebinger, C., 2005. Continental break-up: the East African perspective. Astron. Geophys. 46 (2), 2.16–2.21. https://doi.org/10.1111/j.1468-4004.2005.46216.x.

Ebinger, C.J., Karner, G.D., Weissel, J.K., 1991. Mechanical strength of extended continental lithosphere: constraints from the Western rift system, East Africa. Tectonics 10 (6), 1239–1256. https://doi.org/10.1029/91TC00579.

Ebinger, C.J., Yemane, T., Harding, D.J., Tesfaye, S., Kelley, S., Rex, D.C., 2000. Rift deflection, migration, and propagation: linkage of the Ethiopian and Eastern rifts, Africa. Geol. Soc. Am. Bull. 112 (2), 163–176. https://doi.org/10.1130/0016-7606(2000)112<163:RDMAPL>2.0.CO;2.

Ebinger, C.J., Casey, M., 2001. Continental breakup in magmatic provinces: an Ethiopian example. Geology 29 (6), 527–530. https://doi.org/10.1130/0091-7613(2001)029<0527:CBIMPA>2.0.CO;2.

Feibel, C.S., 1988. Paleoenvironments of Koobi Fora Formation, Turkana Basin, Northern Kenya. PhD thesis. University of Arizona. 327 pp.

Finch, E., Gawthorpe, R., 2017. Growth and interaction of normal faults and fault network evolution in rifts: insights from three-dimensional discrete element modelling. Geol. Soc. (Lond.) Spec. Publ. 439 (1), 219–248. https://doi.org/10.1144/SP439.23.

Ford, M., Hemelsdaël, R., Mancini, M., Palyvos, N., 2017. Rift migration and lateral propagation: evolution of normal faults and sediment-routing systems of the western Corinth rift (Greece). Geol. Soc. (Lond.) Spec. Publ. 439 (1), 131–168. https://doi.org/10.1144/SP439.15.

Gawthorpe, R.L., Leeder, M.R., Kranis, H., Skourtsos, E., Andrews, J.E., Henstra, G.A., Mack, G.H., Muravchik, M., Turner, J.A., Stamatakis, M., 2018. Tectono-sedimentary evolution of the Plio-Pleistocene Corinth rift, Greece. Basin Res. 30 (3), 448–479. https://doi.org/10.1111/bre.12260.

Gawthorpe, R.L., Jackson, C.A.-L., Young, M.J., Sharp, I.R., Moustafa, A.R., Leppard, C.W., 2003. Normal fault growth, displacement localisation and the evolution of normal fault populations: the Hammam Faraun fault block, Suez rift, Egypt. J. Struct. Geol. 25 (6), 883–895. https://doi.org/10.1016/S0191-8141(02)00088-3.

Gawthorpe, R.L., Leeder, M.R., 2000. Tectono-sedimentary evolution of active extensional basins. Basin Res. 12 (3–4), 195–218. https://doi.org/10.1111/j.1365-2117.2000.00121.x.

Goldsworthy, M., Jackson, J., 2001. Migration of activity within normal fault systems: examples from the quaternary of mainland Greece. J. Struct. Geol. 23 (2), 489–506. https://doi.org/10.1016/S0191-8141(00)00121-8.

Guarnieri, P., Brethes, A., Rasmussen, T.M., 2017. Geometry and kinematics of the Triassic rift basin in Jameson Land (East Greenland). Tectonics 36 (4), 602–614. https://doi.org/10.1002/2016TC004419.

Gupta, S., Cowie, P.A., Dawers, N.H., Underhill, J.R., 1998. A mechanism to explain rif-basin subsidence and stratigraphic patterns through fault-array evolution. Geology 26 (7), 595–598.

Haileab, B., Brown, F.H., McDougall, I., Gathogo, P., 2004. Gombe group basalts and initiation of Pliocene deposition in the Turkana depression, northern Kenya and southern Ethiopia. Geol. Mag. 141 (01), 41–53.

Hendrie, D., Kusznir, N., Morley, C., Ebinger, C., 1994. Cenozoic extension in northern Kenya: a quantitative model of rift basin development in the Turkana region. Tectonophysics 236 (1), 409–438.

Huismans, R., Beaumont, C., 2011. Depth-dependent extension, two-stage breakup and cratonic underplating at rifted margins. Nature 473 (7345), 74–78. https://doi.org/10.1038/nature09988.

Knappe, E., Bendick, R., Ebinger, C., Birhanu, Y., Lewi, E., Floyd, M., King, R., Kianji, G., Mariita, N., Temtime, T., Waktola, B., Deresse, B., Musila, M., Kanoti, J., Perry, M., 2020. Accommodation of East African rifting across the Turkana depression. J. Geophys. Res., Solid Earth 125 (2), e2019JB018469. https://doi.org/10.1029/2019JB018469.

Kolawole, F., Phillips, T.B., Atekwana, E.A., Jackson, C.A.-L., 2021. Structural inheritance controls strain distribution during early continental rifting, Rukwa rift. Front. Earth Sci. https://doi.org/10.3389/feart.2021.707869.

Kounoudis, R., Bastow, I.D., Ebinger, C.J., Ogden, C.S., Ayele, A., Bendick, R., Mariita, N., Kianji, G., Wigham, G., Musila, M., Kibret, B., 2021. Body-wave tomographic imaging of the Turkana depression: implications for rifts development and plume-lithosphere interactions. Geochem. Geophys. Geosyst. 22, e2021GC009782.

Kusznir, N.J., Marsden, G., Egan, S.S., 1991. A flexural-cantilever simple-shear/pure-shear model of continental lithosphere extension: applications to the Jeanne d'Arc Basin, Grand Banks and Viking Graben, North Sea. Geol. Soc. (Lond.) Spec. Publ. 56, 41–60.

Kusznir, N.J., Roberts, A.M., Morley, C.K., 1995. Forward and reverse modelling of rift basin formation. Geol. Soc. (Lond.) Spec. Publ. 80, 33–56.

Lavier, L.L., Manatschal, G., 2006. A mechanism to thin the continental lithosphere at magma-poor margins. Nature 440 (7082), 324–328. https://doi.org/10.1038/nature04608.

McCartney, T., Scholz, C.A., 2016. A 1.3 million year record of synchronous faulting in the hangingwall and border fault of a half-graben in the Malawi (Nyasa) rift. J. Struct. Geol. 16, 114–129.

McDougall, I., Brown, F.H., Vasconcelos, P.M., Cohen, B.E., Thiede, D.S., Buchanan, M.J., 2012. New single crystal 40Ar/39Ar ages improve time scale for deposition of the Omo Group, Omo-Turkana Basin, East Africa. J. Geol. Soc. Lond. 169, 213–226.

McDougall, I., Brown, F.H., Fleagle, J.G., 2005. Stratigraphic placement and age of modern humans from Kibish, Ethiopia. Nature 433 (7027), 733–736. https://doi.org/10.1038/nature03258.

Melnick, D., Garcin, Y., Quinteros, J., Strecker, M.R., Olago, D., Tiercelin, J.-J., 2012. Steady rifting in northern Kenya inferred from deformed Holocene lake shorelines of the Suguta and Turkana basins. Earth Planet. Sci. Lett. 331–332, 335–346. https://doi.org/10.1016/j.epsl.2012.03.007.

Morley, C.K., 2020. Early syn-rift igneous dike patterns, northern Kenya rift (Turkana, Kenya): implications for local and regional stresses, tectonics, and magma-structure interactions. Geosphere 16 (3), 890–918. https://doi.org/10.1130/GES02107.1.

Morley, C.K., 2016. Cenozoic structural evolution of the Andaman Sea: evolution from an extensional to a sheared margin. Geol. Soc. (Lond.) Spec. Publ. 431 (1), 39–61.

Morley, C.K., Haranya, C., Phoosongsee, W., Pongwapee, S., Kornsawan, A., Wonganan, N., 2004. Activation of rift oblique and rift parallel pre-existing fabrics during extension and their effect on deformation style: examples from the rifts of Thailand. J. Struct. Geol. 26 (10), 1803–1829. https://doi.org/10.1016/j.jsg.2004.02.014.

Morley, C.K., 2002. Evolution of large normal faults: evidence from seismic reflection data. Am. Assoc. Pet. Geol. Bull. 86 (6), 961–978.

Morley, C.K., Karanja, F., Wescott, W., Stone, D., Harper, R., Wigger, S., Day, R., 1999. Geology and geophysics of the Western Turkana Basins, Kenya. In: Morley, C.K. (Ed.), Geoscience of Rift Systems–Evolution of East Africa. In: AAPG Studies in Geology, vol. 44, pp. 19–54.

Morley, C.K., 1994. Interaction of deep and shallow processes in the evolution of the Kenya rift. Tectonophysics 236, 81–91.

Morley, C.K., Westaway, R., 2006. Subsidence in the super-deep Pattani and Malay basins of Southeast Asia: a coupled model incorporating lower-crustal flow in response to post-rift sediment loading. Basin Res. 18, 51–84.

Muirhead, J.D., Kattenhorn, S.A., Lee, H., Mana, S., Turrin, B.D., Fischer, T.P., Kianji, G., Dindi, E., Stamps, D.S., 2016. Evolution of upper crustal faulting assisted by magmatic volatile release during early-stage continental rift development in the East African rift. Geosphere 12 (6), 1670–1700. https://doi.org/10.1130/GES01375.1.

Muirhead, J.D., Wright, L.J.M., Scholz, C.A., 2019. Rift evolution in regions of low magma input in East Africa. Earth Planet. Sci. Lett. 506, 332–346. https://doi.org/10.1016/j.epsl.2018.11.004.

Naliboff, John B., Buiter, S.J.H., Péron-Pinvidic, G., Osmundsen, P.T., Tetreault, J., 2017. Complex fault interaction controls continental rifting. Nat. Commun. 8 (1), 1179. https://doi.org/10.1038/s41467-017-00904-x.

NEIC, 2020. NEIC earthquake catalogue. National earthquake information centre, on-line bulletin. https://earthquake.usgs.gov/earthquakes/search/.

Nottvedt, A., Gabrielsen, R., Steel, R., 1995. Tectonostratigraphy and sedimentary architecture of rift basins, with reference to the northern North Sea. Mar. Pet. Geol. 12 (8), 881–901.

Nutz, A., Schuster, M., Barboni, D., Gassier, G., Van Bocxlaer, B., Robin, C., Ragon, T., Ghienne, J.-F., Rubino, J.-L., 2020. Plio-Pleistocene sedimentation in West Turkana (Turkana depression, Kenya, East African rift system): paleolake fluctuations, paleolandscapes and controlling factors. Earth-Sci. Rev. 211, 103415. https://doi.org/10.1016/j.earscirev.2020.103415.

Nutz, A., Schuster, M., Boës, X., Rubino, J.-L., 2017. Orbitally-driven evolution of Lake Turkana (Turkana depression, Kenya, EARS) between 1.95 and 1.72 Ma: a sequence stratigraphy perspective. J. Afr. Earth Sci. 125, 230–243.

Nutz, A., Schuster, M., 2016. Stepwise drying of Lake Turkana at the end of the African humid period: a forced regression modulated by solar activity variations? Solid Earth 7, 1609–1618.

Olive, J.-A., Behn, M.D., Malatesta, L.C., 2014. Modes of extensional faulting controlled by surface processes. Geophys. Res. Lett. 41 (19), 6725–6733. https://doi.org/10.1002/2014GL061507.

Owen, R., Renaut, R.W., 1986. Sedimentology, stratigraphy and palaeoenvironments of the Holocene Galana Boi formation, NE Lake Turkana, Kenya. Geol. Soc. (Lond.) Spec. Publ. 25, 311–322.

Pérez-Gussinyé, M., Andrés-Martínez, M., Araújo, M., Xin, Y., Armitage, J., Morgan, J.P., 2020. Lithospheric strength and rift migration controls on synrift stratigraphy and breakup unconformities at rifted margins: examples from numerical models, the Atlantic and South China Sea margins. Tectonics 39 (12), e2020TC006255. https://doi.org/10.1029/2020TC006255.

Peron-Pinvidic, G., Manatschal, G., Osmundsen, P.T., 2013. Structural comparison of archetypal Atlantic rifted margins: a review of observations and concepts. Mar. Pet. Geol. 43, 21–47. https://doi.org/10.1016/j.marpetgeo.2013.02.002.

Phoosongsee, J., Morley, C.K., 2019. Evolution of a major extensional boundary fault system during mupti-phase rifting in the Songkhla Basin, Gulf of Thailand. J. Asian Earth Sci. 172, 1–13.

Pik, R., Marty, B., Carignan, J., Yirgu, G., Ayalew, T., 2008. Timing of East African rift development in southern Ethiopia: implication for mantle plume activity and evolution of topography. Geology 36 (2), 167–170.

Prosser, S., 1993. Rift-related linked depositional systems and their seismic expression. Geol. Soc. (Lond.) Spec. Publ. 71 (1), 35–66. https://doi.org/10.1144/GSL.SP.1993.071.01.03.

Ragon, T., Nutz, A., Schuster, M., Ghienne, J.-F., Ruffet, G., Rubino, J.-L., 2019. Evolution of the northern Turkana depression (East African rift system, Kenya) during the Cenozoic rifting: new insights from the Ekitale Basin (28-25.5 Ma). Geol. J. 54 (6), 3468–3488. https://doi.org/10.1002/gj.3339.

Richter, M.J.A.E., Brune, S., Riedl, S., Glerum, A., Neuharth, D., Strecker, M.R., 2021. Controls on asymmetric rift dynamics: numerical modeling of strain localization and fault evolution in the Kenya rift. Tectonics 40 (5), e2020TC006553.

Rooney, T.O., 2017. The Cenozoic magmatism of East-Africa: Part I — flood basalts and pulsed magmatism. Lithos 286–287, 264–301. https://doi.org/10.1016/j.lithos.2017.05.014.

Rotevatn, A., Jackson, C.A.-L., Tvedt, A.B.M., Bell, R.E., Blækkan, I., 2019. How do normal faults grow? J. Struct. Geol. 125, 174–184. https://doi.org/10.1016/j.jsg.2018.08.005.

Schofield, N., Newton, R., Thackrey, S., Watson, D., Jolley, D., Morley, C., 2020. Linking surface and subsurface volcanic stratigraphy in the Turkana depression of the East African rift system. J. Geol. Soc. https://doi.org/10.1144/jgs2020-110.

Scholz, C.H., Contreras, J.C., 1998. Mechanics of continental rift architecture. Geology 26, 967–970.

Scholz, C.A., Shillington, D.J., Wright, L.J.M., Accardo, N., Gaherty, J.B., Chindandali, P., 2020. Intrarift fault fabric, segmentation, and basin evolution of the lake Malawi (Nyasa) rift, East Africa. Geosphere 16 (5), 1293–1311. https://doi.org/10.1130/GES02228.1.

Schuster, M., Nutz, A., 2018. Lacustrine wave-dominated clastic shorelines: modern to ancient littoral landforms and deposits from the Lake Turkana Basin (East African rift system, Kenya). J. Paleolimnol. 59, 221–243.

Sippel, J., Meessen, C., Cacace, M., Mechie, J., Fishwick, S., Heine, C., Scheck-Wenderoth, M., Strecker, M.R., 2017. The Kenya rift revisited: insights into lithospheric strength through data-driven 3-D gravity and thermal modelling. Solid Earth 8, 45–81.

Stab, M., Bellahsen, N., Pik, R., Quidelleur, X., Ayalew, D., Leroy, S., 2016. Modes of rifting in magma-rich settings: Tectono-magmatic evolution of Central Afar. Tectonics 35 (1), 2–38. https://doi.org/10.1002/2015TC003893.

Stamps, D.S., Calais, E., Saria, E., Hartnady, C., Nocquet, J.-M., Ebinger, C.J., Fernandes, R.M., 2008. A kinematic model for the East African rift. Geophys. Res. Lett. 35 (5). https://doi.org/10.1029/2007GL032781.

Tetreault, J.L., Buiter, S.J.H., 2018. The influence of extension rate and crustal rheology on the evolution of passive margins from rifting to break-up. Tectonophysics 746, 155–172. https://doi.org/10.1016/j.tecto.2017.08.029.

Theunissen, T., Huismans, R.S., 2019. Long-term coupling and feedback between tectonics and surface processes during non-volcanic rifted margin formation. J. Geophys. Res., Solid Earth 124 (11), 12323–12347. https://doi.org/10.1029/2018JB017235.

Ulvrova, M.M., Brune, S., Williams, S., 2019. Breakup without borders: how continents speed up and slow down during rifting. Geophys. Res. Lett. 46 (3), 1338–1347. https://doi.org/10.1029/2018GL080387.

Vétel, W., Le Gall, B., 2006. Dynamics of prolonged continental extension in magmatic rifts: the Turkana rift case study (North Kenya). Geol. Soc. (Lond.) Spec. Publ. 259 (1), 209–233.

Vétel, W., Le Gall, B., Walsh, J.J., 2005. Geometry and growth of an inner rift fault pattern: the Kino Sogo Fault Belt, Turkana rift (North Kenya). J. Struct. Geol. 27 (12), 2204–2222. https://doi.org/10.1016/j.jsg.2005.07.003.

Wedmore, L.N.J., Williams, J.N., Biggs, J., Fagereng, Å., Mphepo, F., Dulanya, Z., Willoughby, J., Mdala, H., Adams, B.A., 2020. Structural inheritance and border fault reactivation during active early-stage rifting along the Thyolo fault, Malawi. J. Struct. Geol. 139, 104097. https://doi.org/10.1016/j.jsg.2020.104097.

Wright, L.J.M., Muirhead, J.D., Scholz, C.A., 2020. Spatiotemporal variations in upper crustal extension across the Different Basement Terranes of the Lake Tan-ganyika rift, East Africa. Tectonics 39 (3), e2019TC006019. https://doi.org/10.1029/2019TC006019.

Ziegler, P.A., Cloetingh, S., 2004. Dynamic processes controlling evolution of rifted basins. Earth-Sci. Rev. 64 (1), 1–50. https://doi.org/10.1016/S0012-8252(03)00041-2.